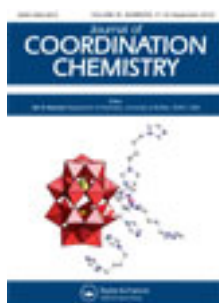


This article was downloaded by: [Renmin University of China]

On: 13 October 2013, At: 10:38

Publisher: Taylor & Francis

Informa Ltd Registered in England and Wales Registered Number: 1072954 Registered office: Mortimer House, 37-41 Mortimer Street, London W1T 3JH, UK



Journal of Coordination Chemistry

Publication details, including instructions for authors and subscription information:

<http://www.tandfonline.com/loi/gcoo20>

Synthesis, characterization, and cytotoxicity of complexes of palladium(II) with 1,4-diaminobutane/1,3-diaminopropane and 4-toluenesulfonyl-L-amino acid dianion

Lili Ma^a, Jinchao Zhang^a, Fangfang Zhang^a, Chao Chen^a,
Luwei Li^a, Shuxiang Wang^a & Shenghui Li^a

^a Key Laboratory of Chemical Biology of Hebei Province, College of Chemistry & Environmental Science, Hebei University, Baoding 071002, P.R. China

Accepted author version posted online: 18 Jul 2012. Published online: 30 Jul 2012.

To cite this article: Lili Ma, Jinchao Zhang, Fangfang Zhang, Chao Chen, Luwei Li, Shuxiang Wang & Shenghui Li (2012) Synthesis, characterization, and cytotoxicity of complexes of palladium(II) with 1,4-diaminobutane/1,3-diaminopropane and 4-toluenesulfonyl-L-amino acid dianion, Journal of Coordination Chemistry, 65:18, 3160-3173, DOI: [10.1080/00958972.2012.713102](https://doi.org/10.1080/00958972.2012.713102)

To link to this article: <http://dx.doi.org/10.1080/00958972.2012.713102>

PLEASE SCROLL DOWN FOR ARTICLE

Taylor & Francis makes every effort to ensure the accuracy of all the information (the "Content") contained in the publications on our platform. However, Taylor & Francis, our agents, and our licensors make no representations or warranties whatsoever as to the accuracy, completeness, or suitability for any purpose of the Content. Any opinions and views expressed in this publication are the opinions and views of the authors, and are not the views of or endorsed by Taylor & Francis. The accuracy of the Content should not be relied upon and should be independently verified with primary sources of information. Taylor and Francis shall not be liable for any losses, actions, claims, proceedings, demands, costs, expenses, damages, and other liabilities whatsoever or howsoever caused arising directly or indirectly in connection with, in relation to or arising out of the use of the Content.

This article may be used for research, teaching, and private study purposes. Any substantial or systematic reproduction, redistribution, reselling, loan, sub-licensing, systematic supply, or distribution in any form to anyone is expressly forbidden. Terms & Conditions of access and use can be found at <http://www.tandfonline.com/page/terms-and-conditions>

Synthesis, characterization, and cytotoxicity of complexes of palladium(II) with 1,4-diaminobutane/1,3-diaminopropane and 4-toluenesulfonyl-L-amino acid dianion

LILI MA, JINCHAO ZHANG*, FANGFANG ZHANG, CHAO CHEN,
LUWEI LI, SHUXIANG WANG* and SHENGHUI LI

Key Laboratory of Chemical Biology of Hebei Province, College of Chemistry
& Environmental Science, Hebei University, Baoding 071002, P.R. China

(Received 6 May 2012; in final form 20 June 2012)

Eight new palladium(II) complexes with 4-toluenesulfonyl-L-amino acid dianion and 1,4-dab/1,3-dap, [Pd(1,4-dab)(TsglyNO)]·H₂O (1), [Pd(1,4-dab)(TsvalNO)] (2), [Pd(1,4-dab)(TsleuNO)] (3), [Pd(1,4-dab)(TsileNO)] (4), [Pd(1,4-dab)(TsserNO)]·0.5H₂O (5), [Pd(1,4-dab)(TspheNO)]·0.5H₂O (6), [Pd(1,4-dab)(TsthrNO)]·H₂O (7), and [Pd(1,3-dap)(TsserNO)] (8), have been synthesized and characterized by elemental analysis, IR, UV, ¹H NMR, and mass spectrometry. Crystal structure of **8** has been determined by X-ray diffraction. The cytotoxicities were tested by MTT assay. The results indicate the complexes exert cytotoxic effects against HL-60 and Bel-7402. The structure–activity relationship suggests that both amino acids and N-containing ligands have important effects on cytotoxicity, but the IC₅₀ values do not show definite correlation with variation of these ligands.

Keywords: Palladium(II) complexes; 4-toluenesulfonyl-L-amino acid dianion; 1,4-Diaminobutane/1,3-Diaminopropane; Cytotoxicity

1. Introduction

In the 1960s, it was discovered that cisplatin inhibited the cell division of *Escherichia coli* [1]. Now, cisplatin is still one of the most successful antineoplastic drugs, used both alone and in combination with other drugs for clinical treatment of numerous types of cancers, including bladder, ovarian, head and neck, testicular, and lung cancers [2–5]. Cisplatin administration is often limited by severe toxic side effects, as well as the intrinsic and acquired resistance possessed by various cancers [6]. To overcome shortcomings of cisplatin, numerous platinum(II)-based compounds have been developed, but only carboplatin and oxaliplatin have received worldwide approval, nedaplatin, lobaplatin, and heptaplatin have gained regionally limited approval, and a few platinum drugs continue to be evaluated in clinical trials. These drawbacks have provided motivation for alternative chemotherapeutic strategies [7–10].

*Corresponding authors. Email: jczhang6970@yahoo.com.cn; wxs@hbu.edu.cn

On the basis of the structural and thermodynamic similarity between platinum(II) and palladium(II) complexes, there is interest in the study of palladium(II) derivatives as potential anticancer drugs [11–13]. Owing to higher lability of palladium *versus* platinum analogs, amino acid ligands, which do not easily dissociate in aqueous solution, have been used to synthesize palladium anticancer complexes [14]. Aromatic N-containing ligands, such as pyridine, quinoline, phenanthroline, and their derivatives, were introduced into metal-based anticancer drugs because of their ability to participate as DNA intercalators [15]. A series of palladium(II) complexes with N-containing ligands and amino acids have shown significant cytotoxic activities. Puthraya *et al.* reported the synthesis and cytotoxicity of palladium(II) complexes $[\text{Pd}(\text{bipy})(\text{AA})]^{n+}$ (where AA is an anion of Cys, Asp, Glu, Met, His, Arg, Phe, Tyr, or Try and $n = 0$ or 1). Among the effective $[\text{Pd}(\text{bipy})(\text{AA})]^{n+}$ complexes, side chain of the amino acids may influence the inhibitory activity. The inhibitory activity decreases as follows: non-polar hydrophobic > polar uncharged > charged side groups [16]. Mital *et al.* reported the synthesis and cytotoxicity of palladium(II) complexes $[\text{Pd}(\text{phen})(\text{AA})]^+$ (where AA is an anion of Gly, Ala, Leu, Phe, Tyr, Try, Val, Pro, or Ser), but the IC_{50} values do not show definite correlation with variation of the amino acid side chains [17]. We previously reported the synthesis and cytotoxicity of some palladium(II) complexes with 4-toluenesulfonyl-L-amino acid dianion and aromatic N-containing ligands. The results indicated that the complexes had cytotoxic effects and selectivity against BGC-823, Bel-7402, KB, and HL-60 cell lines. Moreover, the cytotoxicity of $[\text{Pd}(\text{phen})(\text{TsluNO})] \cdot \text{H}_2\text{O}$ is better than that of cisplatin against BGC-823, Bel-7402, and KB cell lines [18]. Synthesis and cytotoxicity of alky-1,4-butanediamine Pt(II) complexes toward L1210 cells have been reported by Hiroyoshi *et al.* [19]. The structure–activity relationships of the five-, six-, and seven-membered ring structures (which are abbreviated as 5-R, 6-R, and 7-R, respectively) Pt(II) complexes with two different leaving groups (either dichloride or cyclobutane-1,1-dicarboxylate) were summarized. Among these complexes, 7-R had the highest cytotoxic activity. Clinically used platinum-based anticancer drugs have aliphatic N-containing ligands as carrier groups, but the cytotoxicities of mixed-ligand palladium(II) complexes with 1,4-dab/1,3-dap and sulfonyl-L-amino acid dianion have not been reported. In order to further explore the structure–activity relationships and find new metal-based anticancer drugs, the synthesis, characterization, and cytotoxicity of eight new palladium(II) complexes (1–8) with 4-toluenesulfonyl-L-amino acid dianion and 1,4-dab/1,3-dap are reported.

2. Experimental

2.1. Materials

4-Toluenesulfonyl chloride and $\text{K}_2[\text{PdCl}_4]$ were of chemical grade; 1,4-dab and 1,3-dap were of analytical grade. Commercially pure Gly, Val, Leu, Ile, Ser, Phe, and Thr were purchased from Sigma. RPMI-1640 medium, trypsin, and fetal bovine serum were purchased from Gibco. MTT, benzylpenicillin, and streptomycin were from Sigma. Two different human carcinoma cell lines, HL-60 (immature granulocyte leukemia) and Bel-7402 (liver carcinoma), were obtained from American Type Culture Collection.

2.2. Instrumentation and measurement

Elemental analyses were determined on a Elementar Vario EL III elemental analyzer. Electronic spectra in DMF were measured on an UV-3400 Toshniwal spectrophotometer. IR spectra were recorded using KBr pellets and a Perkin-Elmer Model-683 spectrophotometer. ^1H NMR spectra were recorded on a Bruker AVIII 600 NMR spectrometer. Mass spectra were measured by LC-MS apparatus Agilent 1200-6310. Single-crystal X-ray structure was performed on a Bruker SMART APEX II CCD diffractometer. The OD was measured on a microplate spectrophotometer (Bio-Rad Model 680, USA).

2.3. Synthesis of compounds

[Pd(1,4-dab)(TsglyNO)] · H₂O (**1**), [Pd(1,4-dab)(TsvalNO)] (**2**), [Pd(1,4-dab)(TsleuNO)] (**3**), [Pd(1,4-dab)(TsileNO)] (**4**), [Pd(1,4-dab)(TsserNO)] · 0.5H₂O (**5**), [Pd(1,4-dab)(TspheNO)] · 0.5H₂O (**6**), [Pd(1,4-dab)(TsthrNO)] · H₂O (**7**), and [Pd(1,3-dap)(TsserNO)] (**8**) have been prepared by reaction of [Pd(1,4-dab)Cl₂] or [Pd(1,3-dap)Cl₂] with 4-toluenesulfonyl-L-amino acids: TsglyH₂, TsvalH₂, TsleuH₂, TsileH₂, TsserH₂, TspheH₂, or TsthrH₂ in a mixture of CH₃OH/H₂O (figure 1).

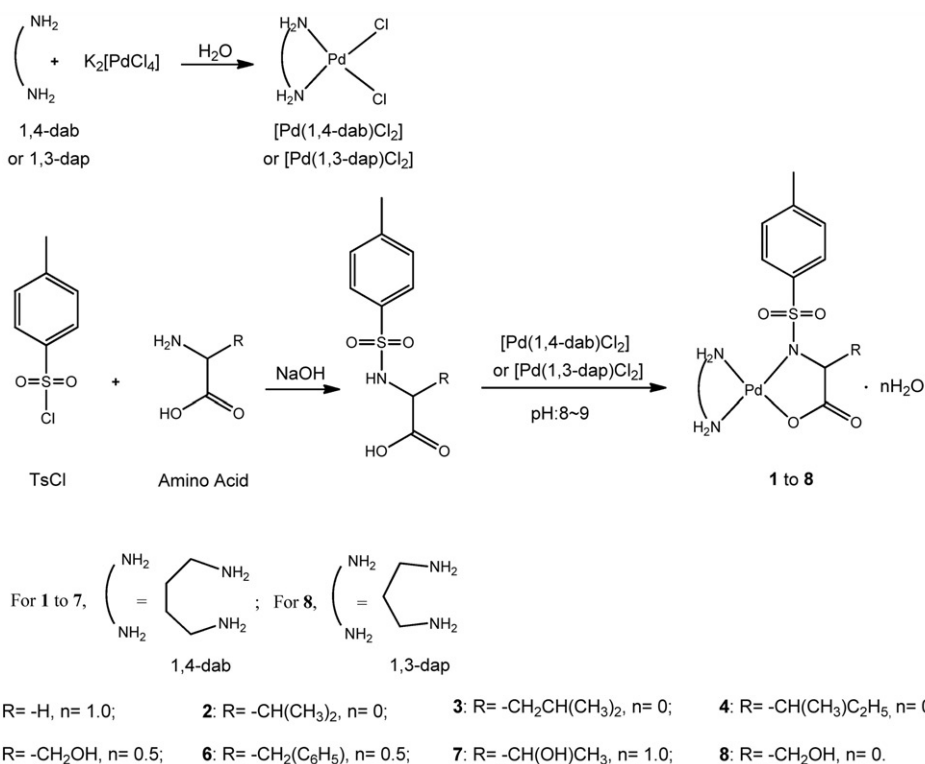


Figure 1. The synthetic route of 1–8.

2.3.1. 4-Toluenesulfonyl-L-amino acids. NaOH (1 mol L⁻¹) of 2.6 mL was added to a rapidly stirred aqueous solution of Gly (195 mg, 2.6 mmol). Another 2.6 mL NaOH (1 mol L⁻¹) was added dropwise after 0.5 h, 4-toluenesulfonyl chloride (500 mg, 2.6 mmol) was added to the solution. This solution was filtered after further 8 h and then was cooled by ice and acidified to pH = 2–3 with HCl (2 mol L⁻¹). The resulting white precipitate was filtered. The collected solid was recrystallized from water and dried to give TsglyH₂: ¹H NMR (600 MHz, DMSO-d₆) δ_(ppm) 7.97 (t, *J* = 6.1 Hz, 1H, NH), 7.68 (d, *J* = 8.2 Hz, 2H, ArH), 7.38 (d, *J* = 8.2 Hz, 2H, ArH), 3.55 (s, 2H, CH₂), 2.38 (s, 3H, CH₃). Melting point: 149.2–150.8°C.

TsvalH₂, TsleuH₂, TsileH₂, TsserH₂, TspheH₂, and TsthrH₂ were carried out similar to TsglyH₂. TsvalH₂: ¹H NMR (600 MHz, CDCl₃) δ_(ppm) 7.72 (d, *J* = 8.3 Hz, 2H, ArH), 7.27 (d, *J* = 8.0 Hz, 2H, ArH), 5.35 (d, *J* = 9.8 Hz, 1H, NH), 3.78 (dd, *J* = 9.8, 4.7 Hz, 1H, CH), 2.16–2.03 (m, 1H, CH), 2.40 (s, 3H, CH₃), 0.94 (d, *J* = 6.8 Hz, 3H, CH₃), 0.87 (d, *J* = 8.2 Hz, 3H, CH₃). Melting point: 146.4–147.7°C. TsleuH₂: ¹H NMR (600 MHz, CDCl₃) δ_(ppm) 7.73 (d, *J* = 8.3 Hz, 2H, ArH), 7.28 (d, *J* = 8.0 Hz, 2H, ArH), 5.33 (d, *J* = 9.7 Hz, 1H, NH), 3.84–4.00 (m, 1H, CH), 2.41 (s, 3H, CH₃), 1.68–1.83 (m, 1H, CH), 1.59–1.42 (m, 2H, CH₂), 0.89 (d, *J* = 6.7 Hz, 3H, CH₃), 0.81 (d, *J* = 6.6 Hz, 3H, CH₃). Melting point: 119.4–120.7°C. TsileH₂: ¹H NMR (600 MHz, CDCl₃) δ_(ppm) 7.72 (d, *J* = 8.1 Hz, 2H, ArH), 7.27 (d, *J* = 8.3 Hz, 2H, ArH), 5.32 (d, *J* = 9.7 Hz, 1H, NH), 3.82 (dd, *J* = 9.7, 4.9 Hz, 1H, CH), 1.86–1.77 (m, 1H, CH), 1.44–1.34 (m, 1H, CH₂), 1.20–1.10 (m, 1H, CH₂), 0.90 (d, *J* = 6.8 Hz, 3H, CH₃), 0.86 (t, *J* = 7.4 Hz, 3H, CH₃). Melting point: 134.1–134.5°C. TsserH₂: ¹H NMR (600 MHz, DMSO-d₆) δ_(ppm) 7.89 (d, *J* = 8.6 Hz, 1H, NH), 7.68 (d, *J* = 7.9 Hz, 2H, ArH), 7.35 (d, *J* = 7.9 Hz, 2H, ArH), 3.80–3.69 (m, 1H, CH), 3.53–3.45 (m, 2H, CH₂), 2.37 (s, 3H, CH₃). Melting point: 223.9–224.9°C. TspheH₂: ¹H NMR (600 MHz, DMSO-d₆) δ_(ppm) 8.18 (d, *J* = 5.0 Hz, 1H, NH), 7.15–7.05 (m, 2H, ArH), 7.36–7.16 (m, 5H, ArH), 7.12 (s, 2H, ArH), 3.82–3.92 (m, 1H, CH), 3.00–2.87 (m, 1H, CH₂), 2.83–2.66 (m, 1H, CH₂), 2.34 (s, 3H, CH₃). Melting point: 150.4–152.9°C. TsthrH₂: ¹H NMR (600 MHz, DMSO-d₆) δ_(ppm) 7.68 (d, *J* = 8.3 Hz, 2H, ArH), 7.53 (d, *J* = 9.2 Hz, 1H, NH), 7.34 (d, *J* = 8.4 Hz, 2H, ArH), 4.00–3.92 (m, 1H, CH), 3.68–3.62 (m, 1H, CH), 2.37 (s, 3H, CH₃), 1.01 (d, *J* = 6.4 Hz, 3H, CH₃). Melting point: 134.5–135.8°C.

2.3.2. Synthesis of precursor complexes. [Pd(1,4-dab)Cl₂] (i) and [Pd(1,3-dap)Cl₂] (ii) were synthesized according to a published procedure [20]. (i) Kelly solid, Yield: 57.3%, Anal. Calcd for C₄H₁₂Cl₂N₂Pd (%): C, 18.10; H, 4.56; N, 10.55. Found (%): C, 18.44; H, 4.12; N, 10.22. (ii) Kelly solid, Yield: 65.4%, Anal. Calcd for C₃H₁₀Cl₂N₂Pd (%): C, 14.33; H, 4.01; N, 11.14. Found (%): C, 14.60; H, 3.68; N, 11.10.

2.3.3. Synthesis of [Pd(1,4-dab)(TsglyNO)]·H₂O (1). [Pd(1,4-dab)Cl₂] (20 mg, 0.075 mmol) was added to a 6 mL CH₃OH/H₂O (volume 2:1) solution of TsglyH₂ (26 mg, 0.113 mmol) and heated to 45°C, adjusted to pH = 8–9 by NaOH (1 mol L⁻¹) solution and then stirred for 3 h. The solution was heated *in vacuo* and concentrated to about 50% of the original volume. Complex **1** separated from the solution after a few days. [Pd(1,4-dab)(TsglyNO)]·H₂O (**1**): Yield: 48.4%. Yellow solid. IR (KBr, cm⁻¹): 1617, 1348, 538, 411. ¹H NMR (600 MHz, DMSO-d₆) δ_(ppm) 7.83 (d, *J* = 8.1 Hz, 2H, ArH), 7.37 (d, *J* = 7.9 Hz, 2H, ArH), 4.53–4.47 (m, 2H, NH₂), 4.40–4.35 (m, 2H, NH₂), 3.37 (s, 2H, CH₂), 2.63–2.58 (m, 2H, CH₂), 2.53–2.52 (m, 2H, CH₂), 2.39 (s, 3H, CH₃),

2.03–1.95 (m, 2H, CH₂), 1.90–1.82 (m, 2H, CH₂). ESI-MS: major peak: 460.7 [M – H₂O + K]⁺. Anal. Calcd for C₁₃H₂₃N₃O₅PdS (%): C, 35.50; H, 5.27; N, 9.55. Found (%): C, 35.34; H, 5.41; N, 9.64.

The syntheses of [Pd(1,4-dab)(TsvalNO)] (2), [Pd(1,4-dab)(TsleuNO)] (3), [Pd(1,4-dab)(TsileNO)] (4), [Pd(1,4-dab)(TsserNO)]·0.5H₂O (5), [Pd(1,4-dab)(TspheNO)]·0.5H₂O (6), [Pd(1,4-dab)(TsthrNO)]·H₂O (7), and [Pd(1,3-dap)(TsserNO)] (8) were carried out in an identical manner.

[Pd(1,4-dab)(TsvalNO)] (2): Yield: 46.3%. Yellow solid. IR (KBr, cm⁻¹): 1636, 1359, 566, 434. ¹H NMR (600 MHz, DMSO-d₆) δ_(ppm) 7.96 (d, *J* = 6.8 Hz, 2H, ArH), 7.33 (d, *J* = 7.2 Hz, 2H, ArH), 4.60–4.52 (m, 1H, NH₂), 4.43–4.35 (m, 1H, NH₂), 4.18–4.08 (m, 2H, NH₂), 3.30 (d, *J* = 4.1 Hz, 1H, CH), 2.68–2.64 (m, 2H, CH₂), 2.64–2.60 (m, 2H, CH₂), 2.36–2.41 (m, 4H, CH₃, CH), 1.92–2.03 (m, 2H, CH₂), 1.83–1.70 (m, 2H, CH₂), 1.19 (d, *J* = 5.9 Hz, 3H, CH₃), 1.07 (d, *J* = 5.9 Hz, 3H, CH₃). ESI-MS: major peak: 486.0 [M + Na]⁺; the relative abundance of isotope peaks match the expected values, i.e., 485.0, 486.0, and 488.0. Anal. Calcd for C₁₆H₂₇N₃O₄PdS (%): C, 41.43; H, 5.87; N, 9.06. Found (%): C, 41.22; H, 5.44; N, 8.71.

[Pd(1,4-dab)(TsleuNO)] (3): Yield: 58.5%. Yellow solid. IR (KBr, cm⁻¹): 1627, 1359, 555, 417. ¹H NMR (600 MHz, DMSO-d₆) δ_(ppm) 7.93 (d, *J* = 7.7 Hz, 2H, ArH), 7.33 (d, *J* = 7.9 Hz, 2H, ArH), 4.52–4.44 (m, 1H, NH₂), 4.39 (m, 1H, NH₂), 4.18–4.09 (m, 2H, NH₂), 3.42 (dd, *J* = 6.0, 4.8 Hz, 1H, CH), 2.74–2.63 (m, 2H, CH₂), 2.63–2.56 (m, 2H, CH₂), 2.38 (s, 3H, CH₃), 2.12–2.06 (m, 1H, CH₂), 2.04–1.98 (m, 1H, CH₂), 1.98–1.91 (d, 1H, CH₂), 1.91–1.83 (d, 1H, CH₂), 1.83–1.74 (m, 2H, CH₂), 1.58–1.52 (m, 1H, CH), 0.96 (d, *J* = 6.6 Hz, 3H, CH₃), 0.89 (d, *J* = 6.6 Hz, 3H, CH₃). ESI-MS: major peak: 500.0 [M + Na]⁺; the relative abundance of isotope peaks match the expected values, i.e., 499.1, 500.0, and 502.0. Anal. Calcd for C₁₇H₂₉N₃O₄PdS (%): C, 42.72; H, 6.12; N, 8.79. Found (%): C, 42.64; H, 5.78; N, 8.57.

[Pd(1,4-dab)(TsileNO)] (4): Yield: 64.9%. Yellow solid. IR (KBr, cm⁻¹): 1644, 1368, 556, 426. ¹H NMR (600 MHz, DMSO-d₆) δ_(ppm) 7.95 (d, *J* = 7.1 Hz, 2H, ArH), 7.33 (d, *J* = 7.4 Hz, 2H, ArH), 4.60–4.50 (m, 1H, NH₂), 4.43–4.35 (m, 1H, NH₂), 4.12–4.07 (m, 2H, NH₂), 3.37 (d, *J* = 3.0 Hz, 1H, CH), 2.70–2.65 (m, 2H, CH₂), 2.63–2.57 (m, 2H, CH₂), 2.38 (s, 3H, CH₃), 2.00–1.90 (m, 1H, CH₂), 1.85–1.69 (m, 5H, CH₂), 1.50–1.41 (m, 1H, CH), 1.13 (d, *J* = 6.0 Hz, 3H, CH₃), 0.89 (t, *J* = 7.2 Hz, 3H, CH₃). ESI-MS: major peak: 500.0 [M + Na]⁺; the relative abundance of isotope peaks match the expected values, i.e., 499.1, 500.0, and 502.0. Anal. Calcd for C₁₇H₂₉N₃O₄PdS (%): C, 42.72; H, 6.12; N, 8.79. Found (%): C, 42.31; H, 5.78; N, 8.51.

[Pd(1,4-dab)(TsserNO)]·0.5H₂O (5): Yield: 59.2%. Yellow solid. IR (KBr, cm⁻¹): 1605, 1399, 556, 401. ¹H NMR (600 MHz, DMSO-d₆) δ_(ppm) 7.96 (d, *J* = 8.2 Hz, 2H, ArH), 7.35 (d, *J* = 7.9 Hz, 2H, ArH), 4.53–4.49 (m, 1H, NH₂), 4.42–4.35 (m, 1H, NH₂), 4.22–4.14 (m, 2H, NH₂), 3.68–3.63 (m, 1H, CH₂), 3.61–3.56 (m, 1H, CH₂), 3.47–3.41 (m, 1H, OH), 3.38–3.36 (t, 1H, CH), 2.69–2.61 (m, 2H, CH₂), 2.53–2.52 (t, *J* = 2.4, 1.8 Hz, 2H, CH₂), 2.39 (s, 3H, CH₃), 2.10–1.98 (m, 2H, CH₂), 1.86–1.80 (m, 2H, CH₂). ESI-MS: major peak: 488.1 [M – 0.5H₂O + K]⁺. Anal. Calcd for C₁₄H₂₄N₃O_{5.5}PdS (%): C, 36.49; H, 5.25; N, 9.12. Found (%): C, 36.49; H, 5.34; N, 9.18.

[Pd(1,4-dab)(TspheNO)]·0.5H₂O (6): Yield: 53.6%. Yellow solid. IR (KBr, cm⁻¹): 1596, 1390, 538, 409. ¹H NMR (600 MHz, DMSO-d₆) δ_(ppm) 7.94 (d, *J* = 8.1 Hz,

2H, ArH), 7.36–7.31 (m, 4H, ArH), 7.29–7.24 (m, 3H, ArH), 4.62–4.44 (m, 1H, NH₂), 4.27–4.23 (m, 1H, NH₂), 3.97–3.88 (m, 2H, NH₂), 3.71–3.68 (dd, $J = 5.4, 4.8$ Hz, 1H, CH), 3.03 (dd, $J = 12.7, 3.7$ Hz, 1H, CH₂), 2.89 (dd, $J = 12.8, 5.7$ Hz, 1H, CH₂), 2.53–2.52 (m, 1H, CH₂), 2.46–2.40 (m, 1H, CH₂), 2.38 (s, 3H, CH₃), 2.37–2.32 (m, 1H, CH₂), 2.23–2.15 (m, 1H, CH₂), 1.75–1.67 (m, 1H, CH₂), 1.64–1.56 (m, 1H, CH₂), 1.53–1.40 (m, 2H, CH₂). ESI-MS: major peak: 534.2 [M – 0.5H₂O + Na]⁺; the relative abundance of isotope peaks match the expected values, i.e., 533.2, 534.2, and 536.2. Anal. Calcd for C₂₀H₂₈N₃O_{4.5}PdS (%): C, 46.11; H, 5.42; N, 8.07. Found (%): C, 46.69; H, 5.12; N, 8.13.

[Pd(1,4-dab)(TsthrNO)]·H₂O (7): Yield: 49.2%. Yellow solid. IR (KBr, cm⁻¹): 1603, 1372, 535, 424. ¹H NMR (600 MHz, DMSO-d₆) δ_(ppm) 7.98 (d, $J = 8.0$ Hz, 2H, ArH), 7.35 (d, $J = 8.1$ Hz, 2H, ArH), 4.58–4.53 (m, 1H, NH₂), 4.44–4.38 (m, 1H, NH₂), 4.37–4.34 (d, $J = 7.5$ Hz, 2H, OH), 4.20–1.28 (d, $J = 6.3$ Hz, 3H, CH₃), 4.10 (m, 2H, NH₂), 3.88–3.82 (m, 1H, CH), 3.34–3.33 (m, 1H, CH), 2.66–2.61 (m, 2H, CH₂), 2.53–2.52 (m, 2H, CH₂), 2.39 (s, 3H, CH₃), 2.10–2.00 (m, 2H, CH₂), 1.85–1.75 (m, 2H, CH₂). ESI-MS: major peak: 487.7 [M – H₂O + Na]⁺; the relative abundance of isotope peaks match the expected values, i.e., 486.5, 487.7, and 490.3. Anal. Calcd for C₁₅H₂₇N₃O₆PdS (%): C, 37.23; H, 5.62; N, 8.68. Found (%): C, 37.49; H, 5.34; N, 8.59.

[Pd(1,3-dap)(TsserNO)] (8): Yield: 68.4%. Yellow crystal. IR (KBr, cm⁻¹): 1592, 1395, 548, 425. ¹H NMR (600 MHz, DMSO-d₆) δ_(ppm) 8.01 (d, $J = 8.0$ Hz, 2H, ArH), 7.35 (d, $J = 7.9$ Hz, 2H, ArH), 4.55–4.48 (m, 1H, OH), 4.42–4.39 (m, 1H, CH), 4.39–4.32 (m, 2H, NH₂), 4.27–4.20 (m, 1H, NH₂), 4.16–4.08 (m, 1H, NH₂), 3.65–3.59 (m, 1H, CH₂), 3.58–3.53 (m, 1H, CH₂), 2.48–2.39 (m, 4H, CH₂), 2.38 (s, 3H, CH₃), 1.70–1.62 (m, 1H, CH₂), 1.54–1.46 (m, 1H, CH₂). ESI-MS: Not found. Anal. Calcd for C₁₃H₂₁N₃O₅PdS (%): C, 35.66; H, 4.83; N, 9.60. Found (%): C, 35.64; H, 4.81; N, 9.93.

2.4. X-ray structure determination of [Pd(1,3-dap)(TsserNO)] (8)

The data collection of **8** was performed on a Bruker SMART APEX II CCD diffractometer equipped with graphite monochromated Mo-K α radiation ($\lambda = 0.71073$ Å) at 296(2) K. Multi-scan absorption corrections were applied using SADABS. The structure was solved by direct methods using the SHELXS-97 program. Refinements on F^2 were performed using SHELXL-97 by full-matrix least-squares with anisotropic thermal parameters for all non-hydrogen atoms. Table 1 lists crystallographic details.

2.5. Cell culture

Two different human carcinoma cell lines, HL-60 and Bel-7402, were cultured in RPMI-1640 medium supplemented with 10% fetal bovine serum, 100 units per mL of penicillin and 100 $\mu\text{g mL}^{-1}$ of streptomycin. Cells were maintained at 37°C in a humidified atmosphere of 5% CO₂ in air.

Table 1. Crystallographic data for **8**.

Formula	C ₁₄ H ₂₅ N ₃ O ₆ PdS
Formula weight	469.83
Temperature (K)	296(2)
Crystal system	Orthorhombic
Space group	<i>P</i> 2 ₁ 2 ₁ 2 ₁
Unit cell dimensions (Å)	
<i>a</i>	7.4231(8)
<i>b</i>	11.1668(12)
<i>c</i>	22.831(2)
Volume (nm ³), <i>Z</i>	1892.5(4), 4
Calculated density (Mg m ⁻³)	1.649
<i>F</i> (000)	960
Crystal size (mm ³)	0.41 × 0.39 × 0.12
θ range for data collection (°)	1.78–33.33
<i>hkl</i> ranges	–10 < <i>h</i> < 11; –6 < <i>k</i> < 17; –32 < <i>l</i> < 34
Data/parameters	6667/231
Goodness-of-fit on <i>F</i> ²	1.125
Final <i>R</i> indices [<i>I</i> > 2 σ (<i>I</i>)]	<i>R</i> ₁ = 0.0284; <i>wR</i> ₂ = 0.0680

2.6. Solutions

The complexes were dissolved in DMSO at 5 mmol L⁻¹ as stock solution and diluted in culture medium at concentrations of 1.0, 10, 100, and 500 μ mol L⁻¹ as working solutions. To avoid DMSO toxicity, the concentration of DMSO was less than 0.1% (v/v) in all experiments.

2.7. Cytotoxicity analysis

The cells harvested from exponential phase were seeded equivalently into a 96-well plate and then the complexes were added to the wells to achieve final concentrations. Control wells were prepared by addition of culture medium. Wells containing culture medium without cells were used as blanks. All experiments were performed in quintuplicate. The MTT assay was performed as described by Mosmann [21]. Upon completion of the incubation for 44 h, stock MTT dye solution (20 mL, 5 mg mL⁻¹) was added to each well. After 4 h incubation, 2-propanol (100 mL) was added to solubilize the MTT formazan. The OD of each well was measured on a microplate spectrophotometer at a wavelength of 570 nm. The IC₅₀ value was determined from a plot of percentage viability against dose of compounds added.

3. Results and discussion

3.1. Characterizations of the complexes

Complex **3** was observed in the ESI-MS as singly charged [M + Na]⁺ ion of *m/z* 500.0. The experimental isotope pattern for this ion matches theoretical predictions (figure 2). ESI-MS of **1**, **2**, and **4–8** are similar to that of **3**. These results provide evidence for the

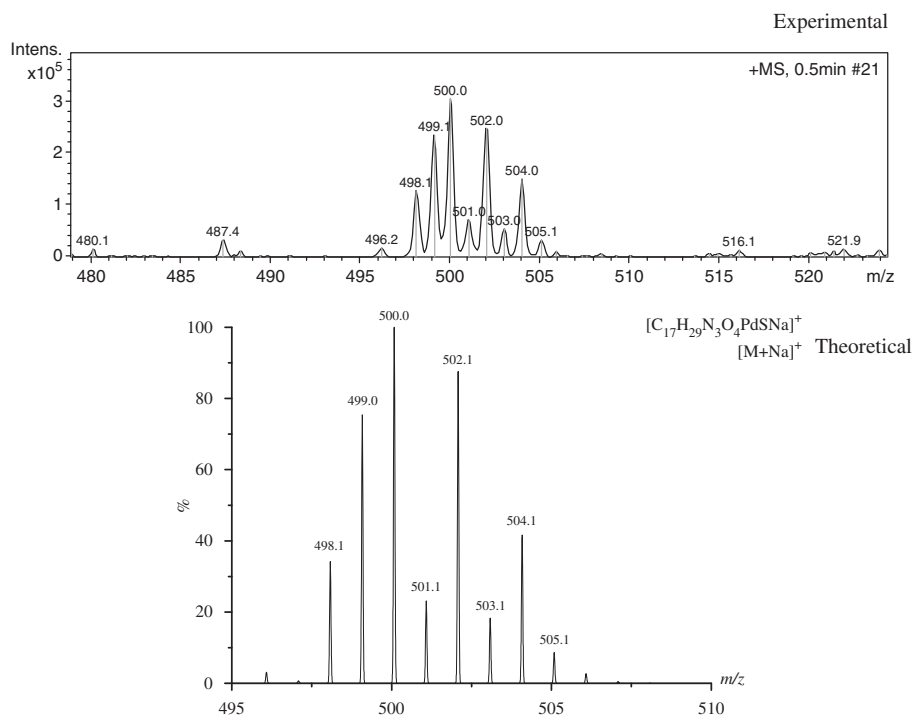


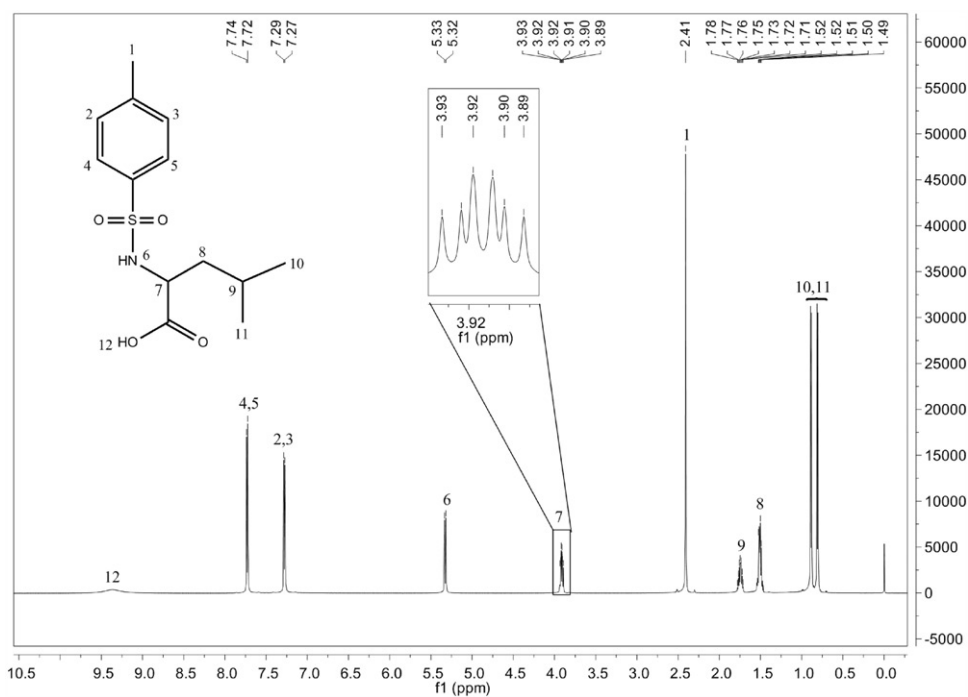
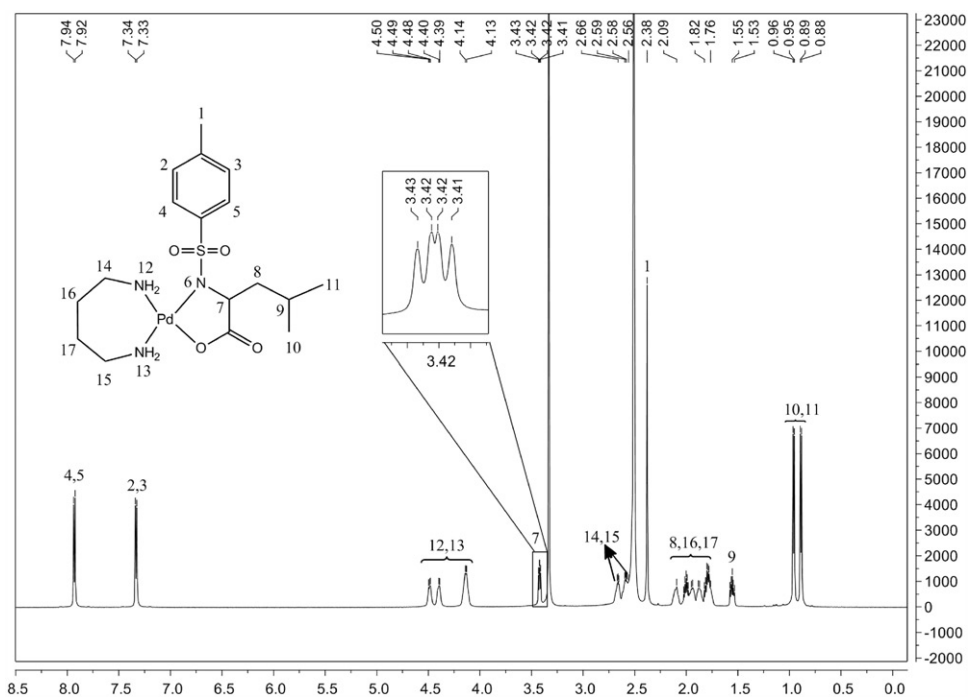
Figure 2. Experimental and theoretical isotope patterns of ESI-MS for **3**.

formation of **1–8**. In addition, there is good agreement between calculated and measured values for the elemental analysis data of **1–8**.

UV-Vis spectroscopy shows that 4-toluenesulfonyl-L-amino acids have shoulders at 267 and 273 nm. After formation of the complexes, the shoulders turn into a single peak at about 268 nm. In addition, there is also a broad LMCT peak at about 350–375 nm for **1–8**, further confirming coordination of palladium(II) with 1,4-dab or 1,3-dap.

The sulfonamide groups of TsglyH₂, TsvalH₂, TsleuH₂, TsileH₂, TsserH₂, TspheH₂, and TsthrH₂ have a strong and sharp ν_{NH} at 3260–3290 cm⁻¹. These peaks disappear for **1–8**, indicating that the sulfonamide has been deprotonated. Deprotonation is further confirmed by the sulfonamide (I) shifting from ~1630 cm⁻¹ to ~1550 cm⁻¹ and the disappearance of the sulfonamide (II). New band at 540 is assigned to $\nu_{\text{Pd-N}}$. The carboxylate of **1–8** shows two bands, an intense antisymmetric stretch $\nu_{(\text{s,COO}^-)}$ and a symmetric stretch $\nu_{(\text{as,COO}^-)}$, at 1620 and 1360 cm⁻¹, respectively. Values of $\Delta\nu_{(\text{COO}^-)}(\nu_{(\text{as,COO}^-)} - \nu_{(\text{s,COO}^-)})$ of **1–8** are 200–270 cm⁻¹, greater than $\Delta\nu_{(\text{COO}^-)}$ of the corresponding sodium carboxylates, so carboxylate may be monodentate through oxygen [22]. This is further confirmed by the appearance of $\nu_{\text{Pd-O}}$. These results are in agreement with the X-ray crystal analysis.

The overall pattern of the ¹H NMR spectra of **1–8** resembles very closely to that of free ligands. TsleuH₂ shows a doublet at $\delta = 3.92$, which is associated with proton of the sulfonamide, but this peak disappears for **3**, showing that sulfonamide is deprotonated (figures 3 and 4). The α -hydrogen of TsleuH₂ is a multiplet, but is a doublet of doublets in the complex, which also shows the deprotonation of sulfonamide. ¹H NMR spectra

Figure 3. ^1H NMR spectra of TsleuH₂.Figure 4. ^1H NMR spectra of 3.

of **1**, **2**, and **4–8** are similar to that of **3**. NMR further confirms that sulfonamide coordinates to Pd(II) through deprotonated sulfonamide nitrogen.

3.2. Structural studies

A view of the molecular structure of [Pd(1,3-dap)(TsserNO)] (**8**) is shown in figure 5. Selected bond lengths and angles are given in table 2. Palladium shows square-planar coordination from two nitrogen atoms of 1,3-dap, one deprotonated sulfonamide nitrogen atom, and one carboxylic oxygen atom. The angle between planar N(2)–Pd(1)–N(3) and planar O(1)–Pd(1)–N(1) is $6.382(76)^\circ$, indicating that the plane Pd(1)–O(1)–N(1)–N(2)–N(3) is slightly distorted. The Pd–N (deprotonated sulfonamide) bond

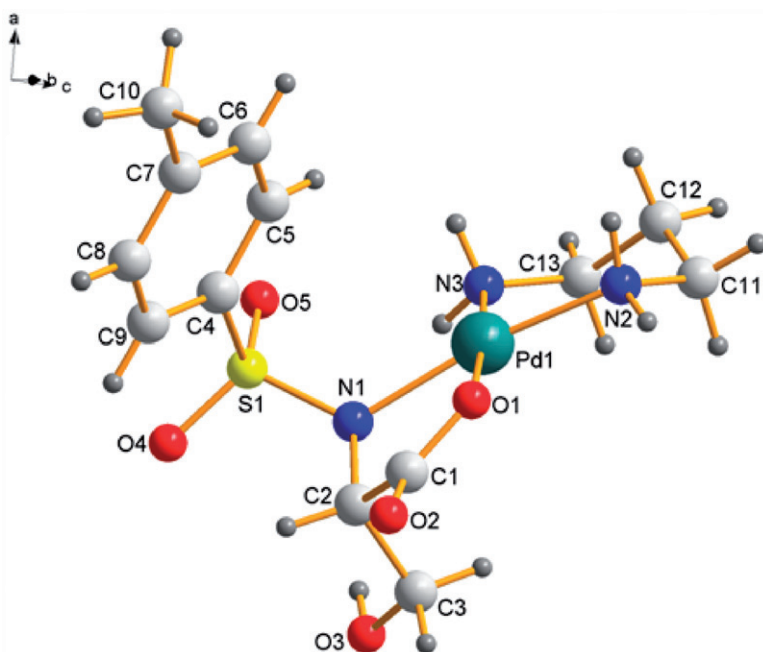


Figure 5. Molecular structure and atom-labeling scheme for **8**.

Table 2. Selected bond lengths (Å) and angles ($^\circ$) for **8**.

Pd(1)–N(3)	2.017(2)
Pd(1)–O(1)	2.0207(18)
Pd(1)–N(1)	2.023(2)
Pd(1)–N(2)	2.041(2)
N(3)–Pd(1)–O(1)	176.23(9)
N(3)–Pd(1)–N(1)	93.86(8)
O(1)–Pd(1)–N(1)	83.09(8)
N(3)–Pd(1)–N(2)	93.75(9)
O(1)–Pd(1)–N(2)	89.52(9)
N(1)–Pd(1)–N(2)	170.42(9)

length (2.023(2) Å) is similar to the Pd–N (1,3-dap) bond lengths (2.017(2) and 2.041(2) Å), while longer than the Pd–O (carboxylic oxygen) bond length (2.0207(18) Å). The similarity of coordinating qualities of the deprotonated amide nitrogen of the carboxylate was reported by Sigel *et al.* as “O-like,” because the deprotonated amide nitrogen and carboxylate are isoelectronic [23]. Cheng *et al.* also reported that deprotonated amide nitrogen was different from ordinary amino nitrogen and its coordination may be “O-like” [24]. In this work, the coordination of the deprotonated sulfonamide nitrogen might be also “O-like.”

3.3. Cytotoxic studies

As shown in figure 6, most complexes exert cytotoxic effects against tested carcinoma cell lines, with selectivity against tested carcinoma cell lines, but none shows higher cytotoxicity than cisplatin. Combined with our previous work [18, 25, 26], the structure–activity relationships are summarized as follows:

- (1) The amino acids have important effects on cytotoxicity. For 1–7 with 1,4-dab and different amino acids, the cytotoxicity against Bel-7402 and HL-60 decreases in the sequences: gly > ser > ile > val > phe > thr > leu and ser > gly > val > thr > phe > leu > ile, respectively. When the amino acid is gly or ser, the complex has the best cytotoxicity. For palladium(II) complexes with bqu and different amino acids, when the amino acid is phe, the complex has the best cytotoxicity against HL-60. When the amino acid is ala, the complex has the best cytotoxicity against Bel-7402 [25]. For palladium(II) complexes with bipy and different amino acids, the cytotoxicity against

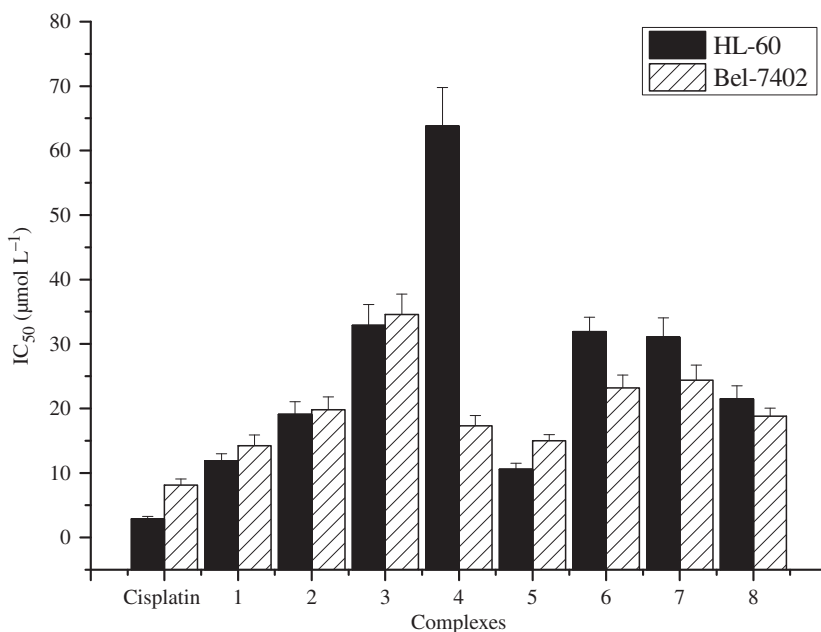


Figure 6. The cytotoxicities of the complexes *in vitro* ($n = 5$).

HL-60 decreases in the sequence: val > phe > ala > leu, but the cytotoxicity against Bel-7402 decreases in the sequence: leu > ala > phe > val [18]. For palladium(II) complexes with phen and different amino acids, when the amino acid is leu, the complex has the best cytotoxicity against HL-60 and Bel-7402 [18]. For palladium(II) complexes with en and different amino acids, the cytotoxicity against HL-60 and Bel-7402 decreases in the same sequence: phe > leu > ala > gly > ser [26]. In addition, the cytotoxicity of $[\text{Pd}(\text{AMBI})(\text{AA})]^{n+}$ (AA is an anion of Gly, Ala, Cys, Met, and Ser) has been reported by El-Sherif. That cytotoxicity against HCT116 and HEP2 decreases in the sequences: met > ser > ala > gly > cys and cys > ser > ala > met > gly, respectively [27].

- (2) The N-containing ligands also have important effects on cytotoxicity. For complexes with val and different N-containing ligands, the cytotoxicity against HL-60 decreases in the sequence: phen > bqu > bipy > 1,4-dab, and the cytotoxicity against Bel-7402 decreases in the sequence: 1,4-dab > bqu > bipy > phen. For complexes with leu and different N-containing ligands, the cytotoxicity against HL-60 decreases in the sequence: phen > en > bqu > bipy > 1,4-dab, while the cytotoxicity against Bel-7402 decreases in the sequence: phen > bipy > en > bqu > 1,4-dab. For complexes with ile and different N-containing ligands, the cytotoxicity against HL-60 decreases in the sequence: bqu > 1,4-dab, while their cytotoxicity against Bel-7402 decreases in the opposite sequence. For the complexes with ser and different N-containing ligands, the cytotoxicity against HL-60 and Bel-7402 decreases in the sequences: 1,4-dab > bqu > 1,3-dap > en, and 1,4-dab > 1,3-dap > bqu > en. For the complexes with phe and different N-containing ligands, the cytotoxicity against HL-60 decreases in the sequence: phen > bqu > en > bipy > 1,4-dab, the cytotoxicity against Bel-7402 decreases in the sequence: phen > bqu > 1,4-dab > en > bipy. In summary, for most of the complexes, aromatic ligands, especially phen, display better anticancer activity [18, 25, 26].

In summary, for palladium(II) complexes with 4-toluenesulfonyl-L-amino acid dianion and N-containing ligands, both amino acids and N-containing ligands have important effects on cytotoxicity and the effect on cytotoxicity is also related to tumor cell type, but the IC_{50} values do not show definite correlation with variation of the amino acid and N-containing ligands.

4. Conclusion

Eight new palladium(II) complexes with 4-toluenesulfonyl-L-amino acid dianion and 1,4-dab/1,3-dap have been synthesized. The cytotoxic experiments indicated that the amino acids had important effects on the cytotoxicity. For palladium(II) complexes with 1,4-dab and different amino acids, when the amino acid is gly or ser, the complex has the best cytotoxicity against Bel-7402 and HL-60, but none of the eight complexes has better cytotoxicity than cisplatin. Current studies are ongoing in our laboratory to gain better insight in the mechanism of action of these palladium(II) complexes, which may be helpful for the design of new metal-based antitumor agents.

Supplementary material

Crystallographic data for the structural analysis of **8** have been deposited with the Cambridge Crystallographic Data Centre, CCDC-830977. Copies of this information may be obtained free of charge from The Director, CCDC, 12 Union Road, Cambridge CB2 1EZ, UK (Fax: +44 1 223 336 033; E-mail: deposit@ccdc.cam.ac.uk or http://www.ccdc.cam.ac.uk).

Acknowledgments

This work was supported by the Special Foundation for State Major New Drug Research Program of China (Grant No. 2009ZX09103-139), the National Basic Research 973 Program (Grant No. 2010CB534913), Hebei Province Nature Science Fund for Distinguished Young Scholars (Grant No. B2011201164), the Nature Science Fund of Hebei Province (Grant No. B2011201135), the Key Basic Research Special Foundation of Science Technology Ministry of Hebei Province (Grant No. 11966412D, 12966418D), and the Key Research Project Foundation of Department of Education of Hebei Province (Grant No. ZD2010142).

References

- [1] B. Rosenberg, L.V. Camp, T. Krigas. *Nat. Rev. Cancer*, **205**, 698 (1965).
- [2] W.P. McGuire, W.J. Hosikins, M.F. Brady, P.R. Kucera, E.E. Partridge, K.Y. Look, D.L. Clarke-Pearson, M. Davidson. *New Engl. J. Med.*, **34**, 1 (1996).
- [3] R. Arriagada, B. Bergman, A. Dunant, T.L. Chevalier, J.P. Pignon. *New Engl. J. Med.*, **350**, 351 (2004).
- [4] N.J. Vogelzang, J.J. Rusthoven, J. Symanowski, C. Denham, E. Kaukel, P. Ruffie, U. Gatzemeier, M. Boyer, S. Emri, C. Manegold, C. Niyikiza, P. Paoletti. *J. Clin. Oncol.*, **21**, 2636 (2003).
- [5] P.G. Rose, B.N. Bundy, E.B. Watkins, J.T. Thigpen, G. Deppe, M.A. Maiman, D.L. Clarke-Pearson, S. Insalaco. *New Engl. J. Med.*, **340**, 1144 (1999).
- [6] M. Kartalou, J.M. Essigmann. *Mutat. Res-Fund. Mol. M.*, **478**, 23 (2001).
- [7] M.A. Jakupec, M. Galanski, V.B. Arion, C.G. Hartinger, B.K. Keppler. *Dalton Trans.*, 183 (2008).
- [8] B.W. Harper, A.M. Krause-Heuer, M.P. Grant, M. Manohar, K.B. Garbutcheon-Singh, J.R. Aldrich-Wright. *Chemistry*, **16**, 7064 (2010).
- [9] E.J. Gao, C. Liu, M. Zhu, H. Lin, Q. Wu, L. Liu. *Anti-Cancer Agents Med. Chem.*, **9**, 356 (2009).
- [10] T.M. Ou, Y.J. Lu, J.H. Tan, Z.S. Huang, K.Y. Wong, L.Q. Gu. *ChemMedChem*, **3**, 690 (2008).
- [11] E.J. Gao, M.C. Zhu, Y. Huang, L. Liu, H.Y. Liu, F.C. Liu, S. Ma, C.Y. Shi. *Eur. J. Med. Chem.*, **45**, 1034 (2010).
- [12] J. Ruiz, J. Lorenzo, C. Vicente, G. López, J.M. López-de-Luzuriaga, M. Monge, F.X. Avilés, D. Bautista, V. Moreno, A. Laguna. *Inorg. Chem.*, **47**, 6990 (2008).
- [13] S. Ray, R. Mohan, J.K. Singh, M.K. Samantaray, M.M. Shaikh, D. Panda, P. Ghosh. *J. Am. Chem. Soc.*, **129**, 15042 (2007).
- [14] A. Matilla, J.M. Tercero, J. Niclós-Gutiérrez, N.H. Dung, B. Viossat, J.M. Pérez, C. Alonso, J.D. Martín-Ramos. *J. Inorg. Biochem.*, **55**, 235 (1994).
- [15] P.C.A. Bruijninx, P.J. Sadler. *Curr. Opin. Chem. Biol.*, **12**, 197 (2008).
- [16] K.H. Puthraya, T.S. Srivastava, A.J. Amonkar, M.K. Adwankar, M.P. Chitnis. *J. Inorg. Biochem.*, **26**, 45 (1986).
- [17] R. Mital, T.S. Srivastava, H.K. Parekh, M.P. Chitnis. *J. Inorg. Biochem.*, **41**, 93 (1991).
- [18] J.C. Zhang, L.W. Li, L.W. Wang, F.F. Zhang, X.L. Li. *Eur. J. Med. Chem.*, **45**, 5337 (2010).
- [19] Y.K. Hiroyoshi Nowatari, H. Hiroshi, O. Kzzuya, E. Hisao, T. Katsutoshi. *Chem. Pharm. Bull.*, **37**, 2406 (1989).
- [20] G. Zhao, H. Lin, Y. Ping, H. Sun, S. Zhu, X.C. Su, Y.T. Chen. *J. Inorg. Biochem.*, **73**, 145 (1999).
- [21] T. Mosmann. *J. Immunol. Methods*, **65**, 55 (1983).

- [22] S. Wang, S. Xiong, Z. Wang, J. Du. *Chem. Eur. J.*, **17**, 8630 (2011).
- [23] H. Sigel. *Inorg. Chem.*, **19**, 1411 (1980).
- [24] Y.Q. Gong, Y.F. Cheng, J.M. Gu, X.R. Hu. *Polyhedron*, **16**, 3743 (1997).
- [25] J.C. Zhang, L.W. Li, L.L. Ma, F.F. Zhang, Z.L. Zhang, S.X. Wang. *Eur. J. Med. Chem.*, **46**, 5711 (2011).
- [26] J.C. Zhang, L.L. Ma, F.F. Zhang, Z.L. Zhang, L.W. Li, S.X. Wang. *J. Coord. Chem.*, **65**, 239 (2012).
- [27] A.A. El-Sherif. *J. Coord. Chem.*, **64**, 2035 (2011).